Critical current of a Josephson junction containing a conical magnet

Gábor B. Halász and J. W. A. Robinson
Department of Material Science, University of Cambridge, Pembroke Street, Cambridge CB2 3QZ, United Kingdom

James F. Annett
H. H. Wills Physics Laboratory, University of Bristol, Royal Fort, Tyndall Avenue, Bristol BS8 1TL, United Kingdom

M. G. Blamire
Department of Material Science, University of Cambridge, Pembroke Street, Cambridge CB2 3QZ, United Kingdom

(Received 16 December 2008; revised manuscript received 17 March 2009; published 8 June 2009)

We calculate the critical current of a superconductor/ferromagnetic/superconductor (S/FM/S) Josephson junction in which the FM layer has a weakened conical magnetic structure composed of an in-plane rotating antiferromagnetic phase and an out-of-plane ferromagnetic component. In view of the realistic electronic properties and magnetic structures that can be formed when conical magnets such as Ho are grown with a polycrystalline structure in thin-film form by methods such as direct current sputtering and evaporation, we have modeled this situation in the dirty limit with a large magnetic coherence length (ξ_f). This means that the electron mean free path is much smaller than the normalized spiral length $\lambda/2\pi$ which in turn is much smaller than ξ_f (with λ as the length a complete spiral makes along the growth direction of the FM). In this physically reasonable limit we have employed the linearized Usadel equations: we find that the triplet correlations are short ranged and manifested in the critical current as a rapid oscillation on the scale of $\lambda/2\pi$. These rapid oscillations in the critical current are superimposed on a slower oscillation which is related to the singlet correlations. Both oscillations decay on the scale of ξ_f. We derive an analytical solution and also describe a computational method for obtaining the critical current as a function of the conical magnetic layer thickness.

DOI: 10.1103/PhysRevB.79.224505 PACS number(s): 74.50.+r, 74.45.+c, 74.20.Rp

I. INTRODUCTION

The interaction of singlet-type superconductors (S) with ferromagnetic (FM) materials in S/FM hybrid systems is a field of extensive and ongoing research (see Refs. 1–3 and references therein). In proximity, the interaction of these competing electron orders is characterized by an oscillating component in the Cooper pair wave function which leads to a number of interesting phenomena: the critical superconducting temperature T_c dependence of S/FM bilayers on FM layer thickness d_f,[4–7] dependence of T_c on the orientation of FM layers in FM′/S/FM″ spin valves[8–13] and S/FM′/FM″ multilayers, and finally the realization of π coupling in S/FM/S Josephson junctions.[14–18]

The standard analysis of the S/FM systems has mostly assumed that the FM is homogeneous and collinear, in which case only the singlet superconducting correlation appears in the theory. Extending this standard approach, theory strongly indicates that if the FM is inhomogeneous and noncollinear, the longer-ranged triplet superconducting correlations should then emerge at the S/FM interface.[1–3] These triplet correlations should then be insensitive to the exchange field of the FM material and as such their proximity range is expected to be similar to that of singlet pairs in a superconductor/normal metal system.

Inhomogeneous magnetization exists in a range of material systems, which can be classified into three categories: (1) magnetic domain walls; (2) ferromagnetic multilayers such as when FM layers are decoupled via a nonmagnetic (NM) spacer to form spin-active devices; and (3) the intrinsically inhomogeneous and noncollinear magnetic materials.

Domain walls were one of the first magnetically inhomogeneous systems to be combined with superconductivity. Although experimental studies of such systems are notoriously challenging because of the need to control the magnetism at the nanometer scale, results and analysis have indicated that domain walls are favorable nucleation sites for superconductivity.[19–23] Theoretically, the emergence of triplet components in junctions containing a single domain wall and or a multidomain ferromagnet (MDFM) have been extensively analyzed.[24,25] Recently, large area S/MDFM/S junctions have been fabricated.[26] In this type of junction, the amplitude of the critical current is expected to decay exponentially with FM layer thickness. If singlet-type electron pairs are scattered into triplet ones at the domain-wall regions, it is expected that for a critical thickness of the MDFM the triplet correlations will dominate over the singlet ones leading to slower decay in the critical current with the MDFM thickness. So far, evidence of a crossover from singlet to triplet-dominated transport in these types of systems is nonexistent.

The second category, the ferromagnetic multilayers, have been combined with superconductors in S/FM′/FM″/S junction form although most studies have been theoretical up to now[27–30] with only a few experiments showing how the Josephson ground state is affected by the orientation of the FM layers.[31,32] The majority of experimental studies have focused on how a superconducting layer is modified by the relative orientation of the FMs. In these systems, however, the triplet superconducting components that exist when the FMs are noncollinear only transmit information about the direction of the magnetic layers.[33,34] To observe a longer-ranged triplet proximity effect, it is thought that the Josephson junction must contain three or more FMs,[30,35] with each offset from the other by an angle $\theta \neq [0, \pi]$ (with π as the

antiparallel configuration). In principle, the angle θ and thus the triplet components could be controlled by the application of an external magnetic field. Unfortunately, the implementation of a large enough change in the angle θ with an applied magnetic field is very difficult to realize without strongly suppressing the superconductivity.

The third category, the intrinsically noncollinear magnets, is potentially one of the simplest systems to combine with a superconductor to experimentally study triplet correlations.[36] Recently,[37] interferometer measurements of superconducting Al coupled to the rare-earth metal Ho have been made. In these Al/Ho/Al junctions, superconducting phase periodic conductance oscillations were observed indicating the presence of a longer-ranged proximity effect when interpreted in the limit of a small coherence length in the Ho relative to the length of a complete spiral λ.[38] It is understood that the triplet correlations were generated at the Al/Ho interface due to a rotating magnetization present there and sustained by a continuous magnetic spiral throughout the length of the Ho. A similar explanation[39–42] was given for a long-ranged proximity effect observed in the half-metal CrO_2.[43] In this system, the triplet current was shown to be insensitive to the strong polarization of the half metal. Spin mixing at the interface is currently the best explanation for the triplet proximity effect observed although a better understanding of the interfaces that can exist in these types of material systems is needed to verify this explanation. For Ho, it is well known that growing it in thin-film form with a magnetic spiral at the interface is difficult to achieve. This again highlights a need to improve our understanding of the likely properties and structures that can arise at the interface of noncollinear magnets, such as Ho, with superconducting materials.

The magnetic structure[44–46] and electronic/thermal properties[45] of the rare-earth Ho are well known. Its magnetic structure has been characterized in bulk, single crystal, and thin-film forms by neutron diffraction, x-ray diffraction, and vibrating sample magnetometery. In thin-film form, the quality of the conical magnetic structure is poorly understood although it is well known that the growth method and growth conditions, crystal forms, and interfacing materials affect the ordering range of the magnetic structure.[44,45]

Long-ranged magnetic ordering in Ho requires a coherent crystal structure in which the c axis is the screw axis with the moments in the basal plane configured into a distorted helix parallel to the c axis. The quality of the Ho (e.g., impurity content and roughness) and the strain at the NM/Ho interface are both important factors in determining the scale of magnetic ordering; for example, substantial intermixing at the NM/FM interface may disturb the growth in the helix which may affect, smear out, or even destroy any triplet correlations. Neutron-diffraction studies on epitaxial (interfacially strained) Nb/Ho bilayer films grown by dc magnetron sputtering[47] at high temperature suggest the presence of an in-plane spiral (antiferromagnetic part) but no out-of-plane pitch (ferromagnetic part) was detected even down to very low temperatures $T \sim 1$ K. This implies that the strain at the Nb/Ho interface is suppressing the ferromagnetic component. Further studies on polycrystalline Nb/Ho/Nb trilayer films have also been made.[48] In these films strain at the Nb/Ho interface is lower and from Josephson-junction-type measurements a weakly conical magnetic structure was confirmed from field-dependent measurements of the junction's critical current as a function of the Ho spacer layer thickness.

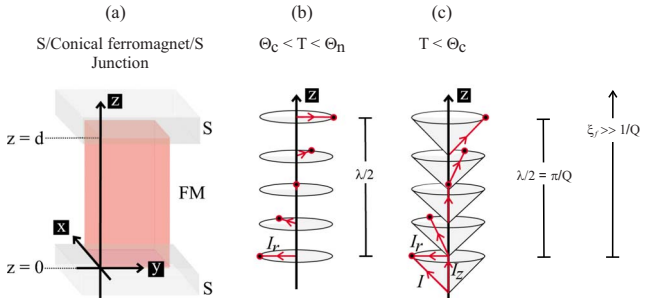

FIG. 1. (Color online) (a) An illustration of two singlet-type superconductors (S) sandwiching a ferromagnet with a conical magnetic structure (Ho). The two magnetic phases of Ho, (b) the in-plane antiferromagnetic spiral phase of Ho below its Néel temperature Θ_n, and (c) the conical magnet phase of Ho below its Curie temperature Θ_c; the antiferromagnetic component I_r rotating in the $\{x,y\}$ plane; the ferromagnetic component I_z pitched toward the z axis; and the resultant magnetization vector $\mathbf{I}$ rotating on the surface of a cone. In the limit considered in this paper, , the ferromagnetic coherence length ξ_f is much larger than $\lambda/2\pi$.

Altogether, the above review shows that although Ho can be grown on top of thick Nb leads with a conical magnetic structure, strain at the interface does weaken the ferromagnetic component possibly implying a weaker magnetism. The motivation behind this work is to complement the currently available theory on S/FM/S junctions with a conical FM weak link by considering the physically reasonable situation (see Sec. III) in which the conical ferromagnetic coherence length ξ_f is much longer than the normalized spiral length $\lambda/2\pi$. Because both ξ_f and $\lambda/2\pi$ are much larger than the electron mean free path l (dirty limit), the S/FM/S junction can be described within the framework of the linearized Usadel equations.

This paper is organized as follows: Sec. II reviews the magnetic and electronic properties of thin-film Ho and outlines the important physical properties of the situation being analyzed in this paper; in Secs. III and IV the general theoretical framework in which we model a Josephson junction containing a conical magnet is described with analytical solutions to obtain the Josephson current explained; in Sec. V we present a computational method for calculating the Josephson current, which is particularly useful to experimentalists.

II. MAGNETIC STRUCTURE AND ELECTRONIC PROPERTIES OF THIN-FILM HOLMIUM

Consider the general structure of a conical magnet which consists of a rotating in-plane magnetization and a constant out-of-plane magnetization [see illustrations in Figs. 1(a)–1(c)]. The in-plane component is effectively an antiferromagnetic (AFM) state which orders itself at the Néel temperature Θ_n, while the out-of-plane component can be considered to be a ferromagnetic phase which orders itself at the Curie temperature of the material. Thus, the strength or ex-

change interaction energy I of the ferromagnetic part is related to the Curie temperature: $I \sim k_B \Theta_c$. The in-plane component completes a full rotation in a distance of λ along the z axis, which implies the distance along z on which the in-plane component rotates in 1 rad is $\lambda/2\pi$. From now on, $\lambda/2\pi$ will be referred to as the normalized spiral length.

In the analysis that follows this section we shall assume that the electron mean-free path ℓ is smaller than both the coherence length of Ho ξ_f and the normalized spiral length $\lambda/2\pi$. For Ho in thin-film form, this limiting situation is justified for the case when it is sputter deposited and polycrystalline.

Polycrystalline thin films of Ho have a large residual resistivity ρ_0 in the $(6-12)\times 10^{-7}$ Ωm range (see Refs. 46 and 48 and references therein). A rough estimate of the electron mean free path for the conduction electrons around 4 K using the relation $\ell = \nu_F m/\rho_0 n e^2$, where ν_F, the Fermi velocity is 1.6×10^6 m/sec,[46] m is the mass of the electron, and n is the number density of free electrons, gives a (0.5–1.0) nm range, which is smaller than both $\xi_f \sim$ (6–7) nm and $\lambda/2\pi \sim$ 1.1 nm.[48] Even in single-crystal form, the resistivity of thin-film Ho is large and around 6×10^{-7} Ωm with an electron mean-free path of $\sim$1.0 nm in the c-axis orientation.

III. GENERAL SOLUTION IN A CONICAL FERROMAGNET

Let us consider a conical ferromagnet FM, the axis of which coincides with the z axis. The magnetization vector and hence the exchange field $\mathbf{I}=(I_x, I_y, I_z)$ has a constant axial component I_z and a radial component I_r, which rotates in the $\{x,y\}$ plane with wave vector $Q=2\pi/\lambda$ as we move along the z direction (see Fig. 1). The x and y components of $\mathbf{I}$ are therefore given by

$$I_x(z) = I_r \cos(Qz) \quad \text{and} \quad I_y(z) = I_r \sin(Qz). \tag{1}$$

In this section we find the solutions for the anomalous Green's function in the conical FM, considering in particular the case of large Q. We assume that the dirty limit is fulfilled, which means that the FM coherence length $(\xi_f = \sqrt{\hbar D_f/|\mathbf{I}|}$ with D_f being the diffusivity of the FM) and the normalized spiral length $\lambda/2\pi$ are both much larger than the electron mean-free path, i.e., $\xi_f, \lambda/2\pi \gg \ell$. If it is also assumed that the anomalous function is sufficiently small in the FM (which is the case if the S/FM interfacial resistance is large enough),[1] we can use the linearized Usadel equation[35]

$$\hbar D_f \frac{d^2\hat{F}(z)}{dz^2} - 2\hbar|\omega|\hat{F}(z) - \mathrm{sgn}(\omega) i[\mathbf{I}(z)\cdot\hat{\boldsymbol{\sigma}}, \hat{F}(z)]_+ = 0, \tag{2}$$

where the anomalous Green's function

$$\hat{F} = f_0 \hat{1} + \mathbf{f}\cdot\hat{\boldsymbol{\sigma}} \tag{3}$$

is a matrix in spin space with $\mathbf{f}=(f_x,f_y,f_z)$, and $\hat{\boldsymbol{\sigma}} = (\hat{\sigma}_x, \hat{\sigma}_y, \hat{\sigma}_z)$ is a vector containing the Pauli matrices. The component f_0 is even, while f_x, f_y, and f_z are odd functions of the frequency ω. The Matsubara frequencies are given by $\omega = (2n+1)\pi k_B T/\hbar$ with $n = 0, \pm 1, \pm 2, \ldots$ at temperature T and $[a,b]_+ = ab+ba$ is the anticommutator. If we substitute expression (3) into Eq. (2) we obtain a set of equations for the four components of the anomalous function $\hat{F}$,

$$\frac{1}{2}\hbar D_f \frac{d^2 f_0(z)}{dz^2} - \hbar\omega f_0(z) - i[\mathbf{I}(z)\cdot\mathbf{f}(z)] = 0, \tag{4}$$

$$\frac{1}{2}\hbar D_f \frac{d^2 f_{x,y,z}(z)}{dz^2} - \hbar\omega f_{x,y,z}(z) - i I_{x,y,z}(z) f_0(z) = 0. \tag{5}$$

Since the symmetric properties of the Usadel equations with respect to ω are trivial, only the case of $\omega > 0$ is treated from now; we already omitted $\mathrm{sgn}(\omega)$ and used ω instead of $|\omega|$ in Eqs. (4) and (5). After putting expression (1) into Eqs. (4) and (5), they can be simplified with the substitution $f_\pm = f_x \pm i f_y$, which yields

$$\frac{d^2 f_0}{dz^2} - 2k_\omega^2 f_0 - i[2k_z^2 f_z + k_r^2 (f_+ e^{-iQz} + f_- e^{iQz})] = 0, \tag{6}$$

$$\frac{d^2 f_\pm}{dz^2} - 2k_\omega^2 f_\pm - 2ik_r^2 f_0 e^{\pm iQz} = 0, \tag{7}$$

$$\frac{d^2 f_z}{dz^2} - 2k_\omega^2 f_z - 2ik_z^2 f_0 = 0. \tag{8}$$

The quantities $k_\omega = \sqrt{\omega/D_f}$ and $k_{z,r} = \sqrt{I_{z,r}/\hbar D_f}$ were also introduced at this step.

By searching a solution for Eqs. (6)–(8) in the form of

$$f_{0,z} = A_{0,z} e^{Kz} \quad \text{and} \quad f_\pm = A_\pm e^{Kz} e^{\pm iQz} \tag{9}$$

with $A_\pm = A'_+ \pm A'_-$, we obtain a set of algebraic equations for the amplitudes A_0, A_z, A'_+, and A'_-

$$(K^2 - 2k_\omega^2)A_0 - 2ik_z^2 A_z - 2ik_r^2 A'_+ = 0, \tag{10}$$

$$-2ik_z^2 A_0 + (K^2 - 2k_\omega^2)A_z = 0, \tag{11}$$

$$-2ik_r^2 A_0 + (K^2 - Q^2 - 2k_\omega^2)A'_+ + 2iKQA'_- = 0, \tag{12}$$

$$2iKQA'_+ + (K^2 - Q^2 - 2k_\omega^2)A'_- = 0. \tag{13}$$

A nontrivial solution only exists for the amplitudes if the determinant of the system is zero; this gives a fourth-order equation for K^2,

$$[(K^2 - 2k_\omega^2)^2 + 4k_z^4][(K^2 - Q^2 - 2k_\omega^2)^2 + 4K^2Q^2] + 4k_r^4(K^2 - 2k_\omega^2)(K^2 - Q^2 - 2k_\omega^2) = 0, \tag{14}$$

which is equivalent to the similar equation obtained by Volkov *et al.*[38] In their paper, they considered the limit in which $k_r, k_z \gg k_\omega, Q$, whereas we take the limit of $Q \gg k_r, k_z, k_\omega$. This limit seems to be appropriate in the case of Ho, which has a conical magnetic structure with $\lambda \approx 6$ nm and therefore $Q \approx 1$ nm^{-1}. The exchange energies I_r and I_z can be estimated from the AFM and FM ordering temperatures; assuming a typical diffusivity $D_f \approx 5\times 10^{-4}$ m^2 s^{-1} and a temperature $T \approx 4$ K, we obtain $k_r \sim 0.2$ nm^{-1}, k_z, and

$k_\omega \sim 0.05\ \mathrm{nm}^{-1}$, which are all much smaller than Q.

In order to make the approximations more transparent, we introduce the dimensionless quantities

$$\lambda = \frac{K^2}{Q^2} \quad \text{and} \quad \epsilon_{r,z,\omega} = \frac{k_{r,z,\omega}^2}{Q^2} \tag{15}$$

with $\epsilon_{r,z,\omega} \ll 1$. Without assuming anything about the relative values of these small numbers, we take the case in which their respective leading terms are on the same order of magnitude; our results are therefore applicable to the general case and the particular cases can be obtained by taking appropriate limits. It turns out that the leading terms in the small quantities $\epsilon_{r,z,\omega}$ are on the orders of ϵ_r^2, ϵ_z, and ϵ_ω, hence we assume for the approximations that $\epsilon_r^2 \sim \epsilon_z \sim \epsilon_\omega$. Two roots of λ are on the order of 1; if we neglect every term smaller than ϵ_r^2 from Eq. (14), we obtain

$$(1+\lambda)^2 = \frac{4\epsilon_\omega}{\lambda}(1+\lambda+2\lambda^2) + \frac{4\epsilon_r^2}{\lambda}(1-\lambda). \tag{16}$$

Since the terms on the right side are $\ll 1$, the left side has to be small, which is only possible if $\lambda \approx -1$. In this case we can substitute $\lambda = -1$ on the right side, hence Eq. (16) reduces to

$$(1+\lambda)^2 + 8\epsilon_\omega + 8\epsilon_r^2 = 0, \tag{17}$$

which gives $\lambda = -1 \pm i\sqrt{8\epsilon_\omega + 8\epsilon_r^2}$. If we only keep the roots of K for which $\mathrm{Re}(K) > 0$ and still neglect the terms smaller than ϵ_r^2, we obtain

$$K_{1,2} = \pm iQ + Q\sqrt{2\epsilon_\omega + 2\epsilon_r^2} \tag{18}$$

for the first two eigenvalues K. These correspond to rapidly oscillating solutions (together with the rotation of the magnetization vector), which decay much more slowly in the negative direction. Since K only appears as K^2 in Eq. (14), the roots with $\mathrm{Re}(K) < 0$ can all be paired up with their respective opposites and give the same solutions decaying in the positive direction. Expression (18) without the term $2\epsilon_r^2$ is equivalent to the result obtained by Bergeret *et al.*[2] for a spiral ferromagnet ($I_z = 0$, hence $\epsilon_z = 0$).

The two remaining roots for λ are on the order of ϵ_r^2; in this case we can treat λ as being small and hence neglect larger powers of it. However, we must keep terms up to the order of ϵ_r^4 in Eq. (14) to obtain the quadratic equation

$$\lambda^2 - 4(\epsilon_r^2 + \epsilon_\omega)\lambda + 4(\epsilon_z^2 + \epsilon_\omega^2 + 2\epsilon_\omega\epsilon_r^2) = 0, \tag{19}$$

which yields $\lambda = 2\epsilon_\omega + 2\epsilon_r^2 \pm 2\sqrt{\epsilon_r^4 - \epsilon_z^2}$. Note that the leading terms are indeed on the orders of ϵ_r^2, ϵ_z, and ϵ_ω, as stated above. Two more eigenvalues K with $\mathrm{Re}(K) > 0$ are obtained,

$$K_{3,4} = Q\sqrt{2\epsilon_\omega + 2\epsilon_r^2 \pm 2\sqrt{\epsilon_r^4 - \epsilon_z^2}}. \tag{20}$$

The behavior of these solutions depends on the relative values of ϵ_z and ϵ_r^2 and now we can consider the two particular cases. If $\epsilon_z > \epsilon_r^2$, the roots $K_{3,4}$ are complex conjugates and solutions (20) describe a slowly decaying oscillation in the negative direction. If $\epsilon_z < \epsilon_r^2$, the roots $K_{3,4}$ are real, which means that $\hat{F}$ decays exponentially without oscillations. This case corresponds to almost in-plane magnetization and contains the limit of the spiral ferromagnet; expression (20) reduces to $K_3 = Q\sqrt{2\epsilon_\omega + 4\epsilon_r^2}$ and $K_4 = Q\sqrt{2\epsilon_\omega}$ if $\epsilon_z = 0$. The solution corresponding to K_4 has zero amplitude in any S/FM system, while K_3 coincides with the value obtained by Bergeret *et al.*[2]

After determining the eigenvalues K we calculate the corresponding eigenvectors, i.e., the relative amplitudes of the different components f_0, f_z, and $f_\pm$ in each solution. Since the roots $K_{1,2}$ given by Eq. (18) appear as a direct consequence of the rotation of the magnetization vector, we expect the components $f_\pm$ to dominate in the corresponding solutions, and hence we choose $A'_{1+} = A'_{2+} = 1$ [A'_{1+} and A'_{2+} are the A'_+ amplitudes appearing in Eqs. (10)–(13) for the solutions corresponding to the roots K_1 and K_2, respectively]. Equation (11) shows that $A_z \ll A_0$ in these cases, while $A_0 \ll A'_+ = 1$ according to Eq. (10). It is valid therefore to take $A_z \approx 0$, then use Eqs. (10) and (13) together with Eq. (18) to obtain $A'_{1-} = -1$, $A'_{2-} = 1$, and $A_{10} = A_{20} = -2i\epsilon_r$ in the leading approximation.

The solutions corresponding to the other two roots $K_{3,4}$ predominantly consist of the components f_0 and f_z, therefore we choose $A_{30} = A_{40} = 1$. Equations (12) and (13) show that $A'_- \ll A'_+ \ll A_0$ in these cases, which implies that $A'_- \approx 0$. Keeping this in mind we can apply Eq. (12) to get $A'_{3+} = A'_{4+} = -2i\epsilon_r$ and Eq. (11) with Eq. (20) to obtain

$$A_{3z} = \frac{i\epsilon_z}{\epsilon_r^2 + \sqrt{\epsilon_r^4 - \epsilon_z^2}} \quad \text{and} \quad A_{4z} = \frac{i\epsilon_z}{\epsilon_r^2 - \sqrt{\epsilon_r^4 - \epsilon_z^2}}. \tag{21}$$

We can again consider the two cases: if $\epsilon_z > \epsilon_r^2$, A_{3z}, and A_{4z} are complex numbers with unit modulus, and $A_{4z} = -A_{3z}^*$. In particular, Eq. (21) reduces to

$$A_{3z} \approx 1 + i\frac{\epsilon_r^2}{\epsilon_z} \quad \text{and} \quad A_{4z} \approx -1 + i\frac{\epsilon_r^2}{\epsilon_z} \tag{22}$$

in the limit of $\epsilon_z \gg \epsilon_r^2$. If $\epsilon_z < \epsilon_r^2$, A_{3z}, and A_{4z} are purely imaginary numbers with $|A_{3z}||A_{4z}| = 1$, they are being approximated as

$$A_{3z} \approx \frac{i\epsilon_z}{2\epsilon_r^2} \quad \text{and} \quad A_{4z} \approx \frac{2i\epsilon_r^2}{\epsilon_z} \tag{23}$$

if $\epsilon_z \ll \epsilon_r^2$. In the limiting case of the spiral ferromagnet ($\epsilon_z \to 0$), $A_{3z} \to 0$, and $|A_{4z}| \to \infty$. The latter means that the solution for $\hat{F}$ corresponding to the root K_4 has only f_z component (and no singlet f_0 component); its amplitude is therefore zero, as already mentioned above.

If we take the eigenvalues K with $\mathrm{Re}(K) < 0$, the corresponding eigenvectors are similar to those corresponding to their opposites; Eqs. (10)–(13) show that the amplitudes A_0, A_z, and A'_+ remain the same if we multiply K by (-1), while A'_- changes sign. According to $A_\pm = A'_+ \pm A'_-$, this means that A_+ and A_- are exchanged. Keeping this in mind, we can write down the general solution for the linearized Usadel Eq. (2) in a conical ferromagnet. If the FM occupies a region of thickness d in the z direction (more specifically, the range $0 < z < d$), the general solution can be written as

$$\hat{F} = \sum_{n=1}^{4} \left[B_n e^{-K_n z} \left(A_{n0}\hat{1} + A_{nz}\hat{\sigma}_z + \frac{1}{2}\sum_{\pm} A_{n\mp} e^{\pm iQz}(\hat{\sigma}_x \mp i\hat{\sigma}_y) \right) + C_n e^{-K_n(d-z)} \left(A_{n0}\hat{1} + A_{nz}\hat{\sigma}_z + \frac{1}{2}\sum_{\pm} A_{n\pm} e^{\pm iQz}(\hat{\sigma}_x \mp i\hat{\sigma}_y) \right) \right], \tag{24}$$

where the eigenvalues K_n and the relative amplitudes A_{n0}, A_{nz}, and $A_{n\pm}=A'_{n+}\pm A'_{n-}$ are given by the expressions obtained in this section. Note that the amplitudes A_{n+} and A_{n-} are exchanged in the terms corresponding to the solutions with $\mathrm{Re}(K)<0$, as mentioned above. The amplitudes B_n and C_n are determined by the boundary conditions at $z=0$ and $z=d$; these are discussed in Sec. IV.

IV. JOSEPHSON CURRENT IN THE S/FM/S JUNCTION

If the regions with $z<0$ and $z>d$ on the two sides of the FM are occupied by two identical half-infinite superconductors S, we obtain a S/FM/S junction. The axis z of the conical FM is perpendicular to the S/FM interfaces (see Fig. 1). The two superconductors have a phase difference of Φ with respect to each other, so the bulk pairing potentials in the left and the right S are given by $\Delta e^{-i\Phi/2}$ and $\Delta e^{i\Phi/2}$ ($\Delta \in \mathbb{R}$). The normal and the anomalous Green functions are $\hat{G}_{L,R}=G_s\hat{1}$ and $\hat{F}_{L,R}=F_s\hat{1}e^{\mp i\Phi/2}$ in the bulk of the left and right superconductors, respectively, where $G_s=\hbar\omega/\sqrt{\hbar^2\omega^2+\Delta^2}$ and $F_s=\Delta/\sqrt{\hbar^2\omega^2+\Delta^2}$. The normal-state conductivities of the S and the FM are σ_s and σ_f, while the interfacial resistance per unit area between the S and the FM is denoted by R. We introduce the dimensionless quantities

$$\gamma = \frac{\sigma_f \xi_s}{\sigma_s \xi_f} \quad \text{and} \quad \gamma_B = \frac{R\sigma_f}{\xi_f}, \tag{25}$$

where $\xi_s=\sqrt{\hbar D_s/2\pi k_B T}$ is the superconducting (quasiparticle) coherence length of the S with D_s being its diffusivity. If the interfacial resistance is large enough, i.e., $\gamma_b \gg \max(1,\gamma)$, we can use rigid boundary conditions at the S/FM interface,[1] we assume that the pairing potential and hence the Green functions are the same at the interface as in the bulk material. Furthermore, because of $\gamma_b \gg 1$ the anomalous function $\hat{F}$ is sufficiently small in the FM, which verifies using the linearized Usadel equations in the FM (see Sec. III).

Assuming that $\gamma_b \gg \max(1,\gamma)$ is true, the rigid boundary conditions are[1]

$$\hat{F}_L = G_s\hat{F}(0) - \gamma_B\xi_f \frac{d\hat{F}(0)}{dz} \tag{26}$$

at the left side of the FM ($z=0$) and

$$\hat{F}_R = G_s\hat{F}(d) + \gamma_B\xi_f \frac{d\hat{F}(d)}{dz} \tag{27}$$

at the right side of the FM ($z=d$). If the FM layer is thick enough ($d \gg \xi_f$), the terms containing $e^{-K_n(d-z)}$ can be neglected from the general solution (24) near $z=0$, while the terms containing $e^{-K_n z}$ can be neglected near $z=d$. In this case we can take the components f_0, f_z, and $f_\pm$ of Eq. (24) at $z=d$ and obtain equations for the amplitudes C_n

$$\frac{\Delta}{\hbar\omega} e^{i\Phi/2} = \sum_{n=1}^{4} C_n A_{n0}(1+\Gamma K_n), \tag{28}$$

$$0 = \sum_{n=1}^{4} C_n A_{nz}(1+\Gamma K_n), \tag{29}$$

$$0 = \sum_{n=1}^{4} C_n A_{n\pm}[1+\Gamma(K_n \pm iQ)], \tag{30}$$

where the notation $\Gamma=\gamma_B\xi_f/G_s$ is used. Similar equations hold for the amplitudes B_n at $z=0$, the only difference is that the sign of the phase $\Phi/2$ in the first term of Eq. (28) is negative. Substituting K_n and $A_{n\pm}$ into Eq. (30) and using $|K_{3,4}| \ll Q$ yields

$$[C_{2,1} - i\epsilon_r(C_3+C_4)] + \Gamma[\pm Q\epsilon_r(C_3+C_4) + k_0 C_{2,1}] = 0, \tag{31}$$

where $k_0=Q\sqrt{2\epsilon_\omega+2\epsilon_r^2}$. Even though $\Gamma Q \gg 1$, $\Gamma Q\epsilon_r \ll 1$ for realistic values of the interfacial resistance; it follows from Eq. (31) that $C_1, C_2 \ll C_3, C_4$, therefore the terms containing C_1 and C_2 can be neglected from Eqs. (28) and (29). Those equations with $A_{30}=A_{40}=1$ take the form of

$$\frac{\Delta}{\hbar\omega} e^{i\Phi/2} = (C_3+C_4) + \Gamma(K_3C_3 + K_4C_4), \tag{32}$$

$$0 = (A_{3z}C_3 + A_{4z}C_4) + \Gamma(A_{3z}K_3C_3 + A_{4z}K_4C_4). \tag{33}$$

In the following we work in the limit of $\epsilon_z \gg \epsilon_r^2$, so we take A_{3z} and A_{4z} given by Eq. (22) to get

$$C_{3,4} = \frac{\Delta e^{i\Phi/2}}{2\hbar\omega(1+K_{3,4}\Gamma)} \left(1 \mp i\frac{\epsilon_r^2}{\epsilon_z}\right), \tag{34}$$

where the expression (20) for the roots $K_{3,4}$ can be approximated as $K_{3,4} \approx Q\sqrt{2\epsilon_\omega+2\epsilon_r^2 \pm 2i\epsilon_z}$ in this case. Substituting C_3 and C_4 into Eq. (31) gives the remaining two amplitudes,

$$C_{1,2} = \frac{\Delta e^{i\Phi/2}\epsilon_r(i \mp \Gamma Q)}{2\hbar\omega(1+k_0\Gamma)} \left(\frac{1 - i\epsilon_r^2/\epsilon_z}{1+K_3\Gamma} + \frac{1 + i\epsilon_r^2/\epsilon_z}{1+K_4\Gamma} \right). \tag{35}$$

The term i can be neglected from the numerator because $\Gamma Q \gg 1$. Furthermore, since K_3 and K_4 are complex conjugates if $\epsilon_z > \epsilon_r^2$, the sum in Eq. (35) can be simplified to

$$C_{1,2} = \mp \frac{\Delta e^{i\Phi/2}\epsilon_r \Gamma Q}{\hbar\omega(1+k_0\Gamma)} \mathrm{Re}\left(\frac{1 - i\epsilon_r^2/\epsilon_z}{1+K_3\Gamma} \right). \tag{36}$$

The results for $B_{3,4}$ and $B_{1,2}$ are the same as those given by Eqs. (34) and (36) with the only difference being a minus sign before $i\Phi/2$ in the phase factor of Δ.

The Josephson current in the S/FM/S junction of area A is given by[35]

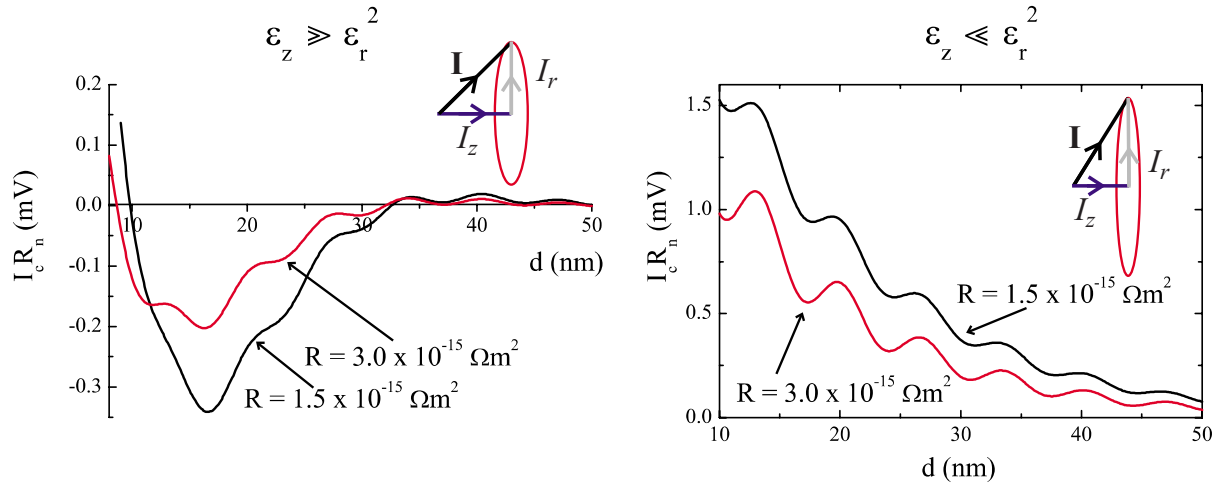

FIG. 2. (Color online) Typical I_cR_n dependence on the thickness d of the FM layer ($\Delta=2.2\times10^{-22}$ J, $Q=9\times10^8$ m^{-1}, $D_f=6\times10^{-4}$ m^2 s^{-1}, $D_s=2.5\times10^{-4}$ m^2 s^{-1}, $\sigma_f=4\times10^6$ $(\Omega\text{m})^{-1}$, and $\sigma_s=6\times10^6$ $(\Omega\text{m})^{-1}$): (left) in the limit of $\epsilon_z\gg\epsilon_r^2$ ($I_r/k_B=I_z/k_B=100$ K) and (right) in the limit of $\epsilon_z\ll\epsilon_r^2$ ($I_r/k_B=130$ K, $I_z/k_B<4$ K) for two different values of the interfacial resistance R.

$$I=\frac{\pi\sigma_f A}{e}k_BT\sum_{\omega>0}\mathrm{Im}\left[\mathrm{Tr}\left(\hat{F}^*(z)\hat{\sigma}_y\frac{d\hat{F}(z)}{dz}\hat{\sigma}_y\right)\right], \quad (37)$$

which can be evaluated in the range $0<z<d$. We can substitute the solution (24) into Eq. (37) and take $z=d$; most terms do not give any imaginary contribution to the trace, hence we obtain

$$I=\frac{\pi\sigma_f A}{e}k_BT\sum_{\omega>0}\mathrm{Im}(S_1+S_2), \quad (38)$$

$$S_1=2\sum_{0,z}\left(\sum_{n=1}^{4}B_n^*A_{n(0,z)}^*e^{-K_n^*d}\sum_{n=1}^{4}C_nA_{n(0,z)}K_n - \sum_{n=1}^{4}C_n^*A_{n(0,z)}^*\sum_{n=1}^{4}B_nA_{n(0,z)}K_ne^{-K_nd}\right), \quad (39)$$

$$S_2=-\sum_{\pm}\left(\sum_{n=1}^{4}B_n^*A_{n\mp}^*e^{-K_n^*d}\sum_{n=1}^{4}C_nA_{n\pm}(K_n\pm iQ) - \sum_{n=1}^{4}C_n^*A_{n\mp}^*\sum_{n=1}^{4}B_nA_{n\pm}(K_n\pm iQ)e^{-K_nd}\right). \quad (40)$$

The first term S_1 mainly contains the solutions corresponding to the eigenvalues $K_{3,4}$, while the second term S_2 is mainly contributed by the solutions corresponding to $K_{1,2}$. By using the values of A_{n0}, A_{nz}, and $A_{n\pm}$ in the limit $\epsilon_z\gg\epsilon_r^2$, the expressions for S_1 and S_2 become

$$S_1=4K_3e^{-K_3d}\left(1+i\frac{\epsilon_r^2}{\epsilon_z}\right)(B_4^*C_3-C_4^*B_3) + 4K_4e^{-K_4d}\left(1-i\frac{\epsilon_r^2}{\epsilon_z}\right)(B_3^*C_4-C_3^*B_4) \quad (41)$$

$$S_2=4k_0[e^{-K_1d}(C_2^*B_1-B_2^*C_1)+e^{-K_2d}(C_1^*B_2-B_1^*C_2)] \quad (42)$$

in the main approximation. Here we neglected the terms containing the small amplitudes A_{10}, A_{20}, $A_{3\pm}$, and $A_{4\pm}$ and used the fact that $|A_{3z}|=|A_{4z}|=1$ if $\epsilon_z>\epsilon_r^2$. By taking $K_2=K_1^*$ and $K_4=K_3^*$ into account, then putting the above-obtained expressions for B_n and C_n into Eqs. (41) and (42) we obtain

$$S_1=4i\sin(\Phi)\frac{\Delta^2}{\hbar^2\omega^2}\mathrm{Re}\left[\frac{K_3e^{-K_3d}}{(1+K_3\Gamma)^2}\left(1-i\frac{\epsilon_r^2}{\epsilon_z}\right)\right], \quad (43)$$

$$S_2=16i\sin(\Phi)\frac{\Delta^2}{\hbar^2\omega^2}\left[\mathrm{Re}\left(\frac{1-i\epsilon_r^2/\epsilon_z}{1+K_3\Gamma}\right)\right]^2 \times\frac{\epsilon_r^2Q^2\Gamma^2k_0e^{-k_0d}}{(1+k_0\Gamma)^2}\cos(Qd). \quad (44)$$

The Josephson current through the S/FM/S junction therefore obeys the formula $I=I_c\sin(\Phi)$, where the critical current I_c is given by

$$I_cR_n=4\pi k_BT\frac{d+2\xi_f\gamma_B}{e}\sum_{\omega>0}\frac{\Delta^2}{\hbar^2\omega^2} \times\left\{\mathrm{Re}\left[\frac{K_3e^{-K_3d}}{(1+K_3\Gamma)^2}\left(1-i\frac{\epsilon_r^2}{\epsilon_z}\right)\right] + \left[\mathrm{Re}\left(\frac{1-i\epsilon_r^2/\epsilon_z}{1+K_3\Gamma}\right)\right]^2\frac{4\epsilon_r^2Q^2\Gamma^2k_0e^{-k_0d}}{(1+k_0\Gamma)^2}\cos(Qd)\right\} \quad (45)$$

with $R_n=(d+2\xi_f\gamma_B)/\sigma_fA$ being the normal-state resistance of the junction.

The dependence of I_cR_n on the thickness d predicted by Eq. (45) is plotted in Fig. 2 (left) for two values of the interfacial resistance R. Both curves show a small rapid oscillation superimposed on a large slow oscillation; they both decay on the scale of the slow oscillation. Comparison between

the two curves demonstrates that an increase in R reduces the current, but makes the rapid oscillations relatively more pronounced.

The first term in Eq. (45) gives the slow oscillation, which is mainly due to the "short-range" singlet and triplet components of the anomalous Green function $\hat{F}$ (i.e., the singlet component f_0 and the triplet component f_z with zero projection on the z axis). Conversely, the second term in Eq. (45) corresponds to the rapid oscillation, which is related to the "long-range" triplet components (i.e., the triplet components $f_\pm$ with projection ± 1 on the z axis). Note that in our case the terms "short range" and "long range" do not mean any difference in the respective decaying lengths; they are only defined like this to be consistent with the notions used in other papers.[35,38]

Unlike the slow oscillation which is also present in a system with a homogeneous FM, the rapid oscillation appears as a direct consequence of the inhomogeneous magnetization. This is shown clearly by the coincidence of its oscillation period and the magnetic spiral wavelength λ. The magnetization changes quickly with respect to the FM coherence length ξ_f, which explains why the amplitude of the rapid oscillation is small compared to that of the slow oscillation.

By taking the limit of $I_r \to 0$ (and hence $\epsilon_r \to 0$), we recover an S/FM/S junction with a homogeneous FM of exchange energy I_z. In this limit, Eq. (45) reduces to

$$I_c R_n = 4\pi k_B T \frac{d + 2\xi_f \gamma_B}{e} \sum_{\omega>0} \frac{\Delta^2}{\hbar^2 \omega^2} \mathrm{Re}\left[\frac{K_3 e^{-K_3 d}}{(1+K_3\Gamma)^2}\right] \quad (46)$$

with the root K_3 taking the form of

$$K_3 = \sqrt{2k_\omega^2 + 2ik_z^2}. \quad (47)$$

This is the standard formula for $I_c R_n$ in a Josephson junction with a homogeneous FM weak link.[1]

The same result is obtained in the limit of $Q \to \infty$ because $\epsilon_r = k_r^2/Q^2 \to 0$ in this case. The amplitude of the rapid oscillation vanishes as Q^{-2}, and hence we recover Eq. (46). This is physically understandable; as the FM coherence length becomes very much larger than the characteristic spiral wavelength, the radial magnetization "averages out" on the scale of ξ_f, which means that the situation is equivalent to $I_r \to 0$.

Now we can return to Eqs. (32) and (33) and take the opposite limit, i.e., where $\epsilon_z \ll \epsilon_r^2$. In this case we use A_{3z} and A_{4z} given by Eq. (23) to obtain different values for the amplitudes B_n and C_n. However, the expression (38) with the same terms S_1 and S_2 still holds for the Josephson current. After substituting the new values of B_n and C_n into Eq. (38) and taking approximations valid in the given limit, we recover $I = I_c \sin(\Phi)$ and obtain

$$I_c R_n = 4\pi k_B T \frac{d + 2\xi_f \gamma_B}{e} \sum_{\omega>0} \frac{\Delta^2}{\hbar^2 \omega^2} \times \left\{ \left[\frac{K_3 e^{-K_3 d}}{(1+K_3\Gamma)^2} - \frac{\epsilon_z^2}{4\epsilon_r^4} \frac{K_4 e^{-K_4 d}}{(1+K_4\Gamma)^2} \right] + \frac{4\epsilon_r^2 Q^2 \Gamma^2 k_0 e^{-k_0 d}}{(1+k_0\Gamma)^2 (1+K_3\Gamma)^2} \cos(Qd) \right\} \quad (48)$$

for the critical current. The roots $K_{3,4}$ given by Eq. (20) can be approximated as $K_3 \approx Q\sqrt{2\epsilon_\omega + 4\epsilon_r^2}$ and $K_4 \approx Q\sqrt{2\epsilon_\omega}$ if $\epsilon_z \ll \epsilon_r^2$.

The $I_c R_n$ dependence on d as given by Eq. (48) is represented in Fig. 2 (right). The rapid oscillation is similar as in the limit of $\epsilon_z \gg \epsilon_r^2$, but the slow oscillation is absent; the other component of I_c decays exponentially without oscillation. The rapid oscillation is still related to the "long-range" triplet components, whereas the exponential decay is related to the "short-range" singlet and triplet components.

In the case between the two limits (where $\epsilon_z \sim \epsilon_r^2$), both expressions (45) and (48) are applicable, but they are not as accurate as when they are used in their respective limiting cases. Since the approximations leading to Eq. (45) are less sensitive than those required for Eq. (48), the former is preferred to be used in such a case.

V. COMPUTATIONAL METHOD FOR CALCULATING THE JOSEPHSON CURRENT

In this section we describe an alternative method for obtaining the Josephson current in the S/FM/S junction; it requires computational power and does not yield an analytical formula, but is exact within the framework of the linearized Usadel equations. The basic steps are the same as in the previous sections: we first solve the linearized Usadel Eq. (2) with the boundary conditions [Eqs. (26) and (27)], then evaluate Eq. (37) at a suitable location.

Let us introduce the formal vector

$$\mathbf{F}(z) = \left(f_0, f_x, f_y, f_z, \frac{df_0}{dz}, \frac{df_x}{dz}, \frac{df_y}{dz}, \frac{df_z}{dz}\right) \quad (49)$$

containing the components of $\hat{F}$ and their respective derivatives with respect to z. We denote the value of this vector $\mathbf{F}_L$ at the right side of the left S (at $z=0$) and $\mathbf{F}_R$ at the left side of the right S (at $z=d$). These consist of the components of $\hat{F}_L$ and $\hat{F}_R$, respectively. $\mathbf{F}_L$ and $\mathbf{F}_R$ can be related through a matrix-type equation and because we know the first four components of both $\mathbf{F}_L$ and $\mathbf{F}_R$, we can use this equation to obtain the remaining four components (the derivatives).

The Josephson current is evaluated with Eq. (37) in the S side of the left S/FM interface; since we calculate the current in the S, we must substitute σ_s instead of σ_f in Eq. (37). By using $f_{xL} = f_{yL} = f_{zL} = 0$ the formula simplifies to

$$I = \frac{2\pi\sigma_s A}{e} k_B T \sum_{\omega>0} \mathrm{Im}\left(f_{0L} \frac{df_{0L}}{dz}\right). \quad (50)$$

By setting the phase difference to $\Phi = \pi/2$ we obtain

$$I_c R_n = 2\pi k_B T \frac{\sigma_s (d + 2\xi_f \gamma_B)}{e\sigma_f} \sum_{\omega>0} \mathrm{Im}\left(f_{0L} \frac{df_{0L}}{dz}\right). \quad (51)$$

Note that the values of f_{0L} and df_{0L}/dz depend on the phase difference Φ, as well as on other parameters describing the junction.

Evaluating df_{0L}/dz requires inverting matrices and taking matrix exponentials, therefore this method does not give an analytical formula like expressions (45) and (48). On the

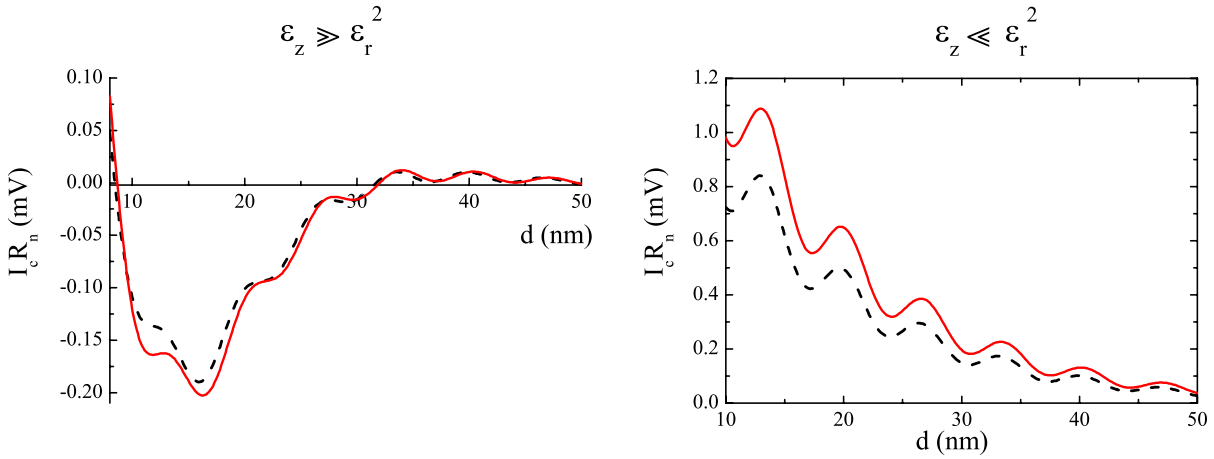

FIG. 3. (Color online) Comparison of the analytical (solid curve) and computational (dashed curve) results for I_cR_n in the function of the thickness d: (left) in the limit of $\epsilon_z \gg \epsilon_r^2$ and (right) in the limit of $\epsilon_z \ll \epsilon_r^2$. The parameters used are identical to those in Fig. 2 with $R = 3.0 \times 10^{-15}$ Ωm^2.

other hand, it gives the right result in the more general case, even if Q is not large [in which case neither Eq. (45) nor Eq. (48) is applicable]. This method can also be used to check analytical results; in our case it seems that within their respective ranges, Eqs. (45) and (48) show good coincidence with the results obtained by the computational method (see Fig. 3).

VI. SUMMARY

We have calculated the Josephson current in a superconductor/ferromagnetic/superconductor junction in which the ferromagnet has a conical magnetic structure. In view of the realistic interfaces that can exist between thin-film superconductors (Al, Pb, and Nb being the elements typically used) and thin films of conical magnets such as Ho, we have extended the problem to a regime in which the ferromagnetic coherence length is long compared to the electron mean-free path and the normalized spiral length of the magnetic spiral.

From the materials point of view, the dirty-limit model we present is physically reasonable and most applicable for when the Ho thin film is polycrystalline. The electron mean-free path of thin film Ho is <1.0 nm and its normalized spiral length <1.1 nm, whereas the coherence length in such films has recently been determined to be in the 6–7 nm range.[48]

In this new situation, we have shown that the Josephson current is highly sensitive to the length of the conical ferromagnet λ with the current containing a rapidly oscillating component in the function of the total conical magnetic thickness. These rapid oscillations are superimposed on a much slower oscillation which has a longer wavelength. The longer oscillation is directly linked to the strength of the ferromagnetic component and mainly depends on the singlet part of the anomalous Green function $\hat{F}$. The sign of the longer oscillation varies with multiple phase transitions from 0 to π which depend on the thickness of the magnetic layer. The rapid oscillations are linked to the triplet components $f_{\pm}$ of the anomalous Green function $\hat{F}$. Although of a shorter wavelength to the slower oscillations, this rapid oscillation also decays on the scale of the magnetic coherence length.

The main feature of the results presented in this paper is that the Josephson coupling through a conical ferromagnet may not be long ranged as previously expected. In the limit considered, we have shown that the proximity effect is short with a length scale comparable to that of the proximity effects in a weak and collinear ferromagnet. Thus, the theory explained in this paper is complementary to previous studies[36–38] which assume that the magnetism of thin-film conical magnets is comparable to the magnetism of conical magnets in bulk single-crystal form.

From the experimental view, the theory presented in this paper is directly applicable to situations in which two singlet-type superconductors are coupled via a rare-earth conical magnet (e.g., Ho). The experiment should be designed in such a way that the current flowing through the superconductor/ferromagnetic/superconductor junction is restricted to the growth direction of the conical magnet, e.g., along the z axis, such as in the case illustrated in Fig. 1(a). For similar experimental situations, see Refs. 18 and 49.

ACKNOWLEDGMENTS

We are grateful to the Engineering and Physical Sciences Research Council for supporting this research through Grant No. EP/F016611. J.W.A.R. acknowledges financial support from St. John's College, Cambridge, and G.B.H. kindly acknowledges J. Driscoll of Trinity College, Cambridge, for supporting his research.

[1] A. I. Buzdin, Rev. Mod. Phys. **77**, 935 (2005).
[2] F. S. Bergeret, A. F. Volkov, and K. B. Efetov, Phys. Rev. B **64**, 134506 (2001).
[3] F. S. Bergeret, A. F. Volkov, and K. B. Efetov, Rev. Mod. Phys. **77**, 1321 (2005).
[4] J. S. Jiang, D. Davidović, D. H. Reich, and C. L. Chien, Phys. Rev. Lett. **74**, 314 (1995).
[5] Th. Mühge, N. N. Garif'yanov, Yu. V. Goryunov, G. G. Khaliullin, L. R. Tagirov, K. Westerholt, I. A. Garifullin, and H. Zabel, Phys. Rev. Lett. **77**, 1857 (1996).
[6] M. Vélez, M. C. Cyrille, S. Kim, J. L. Vicent, and I. K. Schuller, Phys. Rev. B **59**, 14659 (1999).
[7] P. Koorevaar, Y. Suzuki, R. Coehoorn, and J. Aarts, Phys. Rev. B **49**, 441 (1994).
[8] V. Peña, Z. Sefrioui, D. Arias, C. Leon, J. Santamaria, J. L. Martinez, S. G. E. te Velthuis, and A. Hoffmann, Phys. Rev. Lett. **94**, 057002 (2005).
[9] I. C. Moraru, W. P. Pratt, Jr., and N. O. Birge, Phys. Rev. Lett. **96**, 037004 (2006).
[10] A. Yu. Rusanov, S. Habraken, and J. Aarts, Phys. Rev. B **73**, 060505(R) (2006).
[11] J. Y. Gu, C.-Y. You, J. S. Jiang, J. Pearson, Ya. B. Bazaliy, and S. D. Bader, Phys. Rev. Lett. **89**, 267001 (2002).
[12] A. Potenza and C. H. Marrows, Phys. Rev. B **71**, 180503(R) (2005).
[13] D. Stamopoulos, E. Manios, and M. Pissas, Phys. Rev. B **75**, 014501 (2007).
[14] V. V. Ryazanov, V. A. Oboznov, A. Yu. Rusanov, A. V. Veretennikov, A. A. Golubov, and J. Aarts, Phys. Rev. Lett. **86**, 2427 (2001).
[15] T. Kontos, M. Aprili, J. Lesueur, F. Genêt, B. Stephanidis, and R. Boursier, Phys. Rev. Lett. **89**, 137007 (2002).
[16] C. Bell, R. Loloee, G. Burnell, and M. G. Blamire, Phys. Rev. B **71**, 180501(R) (2005).
[17] V. A. Oboznov, V. V. Bol'ginov, A. K. Feofanov, V. V. Ryazanov, and A. I. Buzdin, Phys. Rev. Lett. **96**, 197003 (2006).
[18] J. W. A. Robinson, S. Piano, G. Burnell, C. Bell, and M. G. Blamire, Phys. Rev. Lett. **97**, 177003 (2006).
[19] F. S. Bergeret, A. F. Volkov, and K. B. Efetov, Phys. Rev. Lett. **86**, 4096 (2001).
[20] A. Yu. Aladyshkin, A. I. Buzdin, A. A. Fraerman, A. S. Melnikov, D. A. Ryzhov, and A. V. Sokolov, Phys. Rev. B **68**, 184508 (2003).
[21] Z. Yang, M. Lange, A. Volodin, R. Szymczak, and V. V. Moshchalkov, Nature Mater. **3**, 793 (2004).
[22] W. Gillijns, A. Yu. Aladyshkin, M. Lange, M. J. Van Bael, and V. V. Moshchalkov, Phys. Rev. Lett. **95**, 227003 (2005).
[23] L. Y. Zhu, T. Y. Chen, and C. L. Chien, Phys. Rev. Lett. **101**, 017004 (2008).
[24] A. F. Volkov and K. B. Efetov, Phys. Rev. B **78**, 024519 (2008).
[25] A. I. Buzdin and A. S. Melnikov, Phys. Rev. B **67**, 020503(R) (2003).
[26] T. S. Khaire, W. P. Pratt, Jr., and N. O. Birge, Phys. Rev. B **79**, 094523 (2009).
[27] Y. S. Barash, I. V. Bobkova, and T. Kopp, Phys. Rev. B **66**, 140503(R) (2002).
[28] T. Yu. Karminskaya, M. Yu. Kupriyanov, and A. A. Golubov, JETP Lett. **87**, 570 (2008).
[29] V. N. Krivoruchko and E. A. Koshina, Phys. Rev. B **64**, 172511 (2001).
[30] A. F. Volkov, F. S. Bergeret, and K. B. Efetov, Phys. Rev. Lett. **90**, 117006 (2003).
[31] A. Vedyayev, C. Lacroix, N. Pugach, and N. Ryzhanova, Europhys. Lett. **71**, 679 (2005).
[32] C. Bell, G. Burnell, C. W. Leung, E. J. Tarte, D.-J. Kang, and M. G. Blamire, Appl. Phys. Lett. **84**, 1153 (2004).
[33] P. Cadden-Zimansky, Ya. B. Bazaliy, L. M. Litvak, J. S. Jiang, J. Pearson, J. Y. Gu, C.-Y. You, M. R. Beasley, and S. D. Bader, Phys. Rev. B **77**, 184501 (2008).
[34] J. W. A. Robinson, G. B. Halász, A. I. Buzdin, and M. G. Blamire, arXiv:0808.0166 (unpublished).
[35] M. Houzet and A. I. Buzdin, Phys. Rev. B **76**, 060504(R) (2007).
[36] J. Linder, T. Yokoyama, and P. Sudbø, Phys. Rev. B **79**, 054523 (2009).
[37] I. Sosnin, H. Cho, V. T. Petrashov, and A. F. Volkov, Phys. Rev. Lett. **96**, 157002 (2006).
[38] A. F. Volkov, A. Anishchanka, and K. B. Efetov, Phys. Rev. B **73**, 104412 (2006).
[39] M. Eschrig and T. Löfwander, Nat. Phys. **4**, 138 (2008).
[40] M. Eschrig, J. Kopu, J. C. Cuevas, and G. Schön, Phys. Rev. Lett. **90**, 137003 (2003).
[41] Y. Asano, Y. Sawa, Y. Tanaka, and A. A. Golubov, Phys. Rev. B **76**, 224525 (2007).
[42] A. V. Galaktionov, M. S. Kalenkov, and A. D. Zaikin, Phys. Rev. B **77**, 094520 (2008).
[43] R. S. Keizer, S. T. B. Goennenwein T. M. Klapwijk, G. Miao, G. Xiao, and A. Gupta, Nature (London) **439**, 825 (2006).
[44] W. C. Koehler, J. W. Cable, H. R. Child, M. K. Wilkinson, and E. O. Wollan, Phys. Rev. **158**, 450 (1967).
[45] S. Chikazumi, *Physics of Ferromagnetism* (Oxford University Press, England, 1997).
[46] K. V. Rao, Phys. Rev. Lett. **22**, 943 (1969).
[47] J. Witt, S. Langridge, T. Hase, and M. G. Blamire (unpublished).
[48] J. Witt, J. W. A. Robinson, and M. G. Blamire (unpublished).
[49] C. Bell, G. Burnell, D.-J. Kang, R. H. Hadfield, M. J. Kappers, and M. G. Blamire, Nanotechnology **14**, 630 (2003).